CHEMISTRY OF MATERIALS

Article

pubs.acs.org/cm

Ionically Self-Assembled Clustomesogen with Switchable Magnetic/Luminescence Properties Containing $[Re_6Se_8(CN)_6]^{n-}$ (n = 3, 4) Anionic Clusters

Yann Molard,*[,†] Alexandra Ledneva,[†,‡] Maria Amela-Cortes,[†] Viorel Cîrcu,[§] Nikolai G. Naumov,[‡] Cristelle Mériadec,[⊥] Franck Artzner,[⊥] and Stéphane Cordier[†]

[†]UMR "Sciences Chimiques de Rennes", UR1-CNRS 6226, Equipe Chimie du Solide et Matériaux, and [⊥]UMR "Institut de Physique de Rennes", UR1-CNRS 6251, Université de Rennes 1, Campus de Beaulieu, CS 74205, 35042 Rennes Cedex, France

[‡]Nikolaev Institute of Inorganic Chemistry, Siberian Branch of the Russian Academy of Sciences, 3 Acad. Lavrentiev pr., 630090 Novosibirsk, Russia

[§]Department of Inorganic Chemistry, University of Bucharest, Dumbrava Rosie 23, Bucharest 020464, sector 2, Romania

Supporting Information

ABSTRACT: Octahedral anionic rhenium clusters are obtained by high-temperature solid-state chemistry synthesis as single crystals or powders within which their charge is counter balanced by alkali cations. The ceramic-like behavior of the solid-state Re_6 based inorganic compound limits strongly their use in functional devices. We present herein a facile route to introduce these anionic clusters in a self-organized hybrid organic−inorganic material. By replacing alkali countercations by mesogenic organic ones, polarized optical microscopy (POM), DSC, X-ray, magnetic, fluorescence, and cyclic voltammetry techniques confirm that a lyotropic and thermotropic liquid crystal material, able to switch reversibly from a bright red NIR luminescent form to a magnetic green-colored one, is obtained.

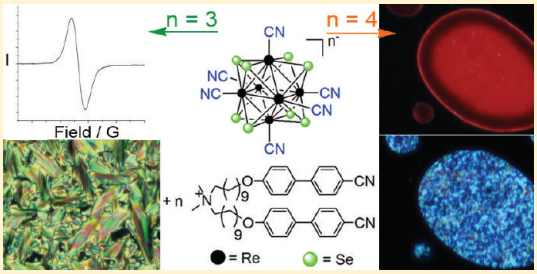

KEYWORDS: *cluster compounds, hybrid materials, luminescence, liquid crystals*

INTRODUCTION

Liquid crystals (LC) are nowadays extensively used in high technology materials found in low-power flat-panel displays but are also found in diverse applications such as temperature sensing, solvents in chemical reactions, or in the fields of spectroscopy, holography, or biomedical, etc. In addition to their exceptional self-assembling abilities in the solid state or in solution, properties such as luminescence, redox states, and/or magnetism can be incorporated inside LC by introducing a metallic center in its core, leading to functional or multifunctional materials.[1]

Clustomesogens, liquid-crystalline material containing metallic cluster complexes, are an attractive emerging class of multifunctional molecular hybrid nanomaterial.[2] As metallomesogens,[1a,c,3] they combine the specific properties of metallic clusters (magnetic, electronic, luminescence), related to the number of metallic electrons available for metal−metal bonds (VEC),[4] with the anisotropy-related properties of liquid crystals. However, in contrast to luminescent metallomesogen previously described, their luminescence properties are not influenced by their supramolecular organization and only poorly by their surrounding ligands. This peculiar point is of interest since known properties can be directly imported in the desired hybrid matrices. Indeed, nanosized octahedral metallic clusters found in $[M_6Q^i_8X^a_6]^{n-}$ anionic units (M = Mo, W, or Re; Q = chalcogen/halogen; X = halogen; i = inner, a = apical, $2 \leq n \leq 4$) are highly emissive in the red-NIR area with photoluminescence quantum yields up to 0.23,[5] displaying tenth of microseconds excited state lifetimes.[4b,5,6] They are obtained as powders or single crystals by high-temperature solid-state synthesis in silica containers. Within the solid, the charge balance is generally assumed by alkali or divalent cations and the anionic $[M_6Q^i_8X^a_6]^{n-}$ units can either share common ligands with other units or be discrete. Unfortunately, the ceramic-like behavior of the solid state Re_6 based inorganic compound limits strongly their interest and potential use in the design of functional devices, commanding new strategies of integration to be explored. Thus, many studies have been devoted these last decades to the solubilization of cluster-based inorganic solids in aqueous or organic solution, in order to introduce clusters, as molecular species, in the playgrounds of organometallic, coordination, and hybrid materials chemistries.[7] $A_n[M_6Q^i_8X^a_6]$ inorganic salts (A = alkali or divalent cation)[7b,8] can become fairly soluble in organic media after a cationic metathesis reaction which consists in replacing the inorganic counter cations by organic ones.[7b,9] This solubilization allows their direct integration in functional materials[7d−f] or their

Received: June 6, 2011
Revised: October 26, 2011
Published: November 10, 2011

modification with organic moieties giving hybrid building blocks where organic ligands are orthogonally arranged around the cluster core.[7b,c,10] Recently, we described the covalent grafting of six promesogenic organic ligands in the apical positions of a Mo_6 cluster core.[2a] This first example of clustomesogen self-organizes in layers (smectic phase) on a large temperature range (22−103 °C). Taking into consideration the size of metallic cluster cores (around 1 nm), their negative charge and their particular redox properties, we decided to explore a new route based on the ionic self-assembly[11] (ISA) strategy to generate clustomesogens. This strategy appears as very interesting for its cost-effectiveness and has already proven to be powerful to generate easily liquid crystal phases by combining specific organic cations with polyanionic inorganic entities such as polyoxometalate[12] or $[Ni_3P_3S_{12}]^{3-}$ complexes.[13] Depending on the nature of the constituting metal atoms, inner (Q^i) and apical (X^a) ligands, the cluster charge and the value of the oxidation potential can be adjusted at will. For instance, Re_6 based clusters of formula $[Re_6Se_8(CN)_6]^{n-}$ (n = 3, 4) show a low oxidation potential and can be reversibly switched from an orange colored form (n = 4, VEC = 24) with red-NIR luminescence properties, to a stable and magnetic green colored species (n = 3, VEC = 23).[14] Such modification can be easily implemented by both chemical and electrochemical oxidation, that can be useful for color, luminescence and magnetic switching. Thus, we suspected that, by using a mixture containing either a 4− or 3− charged anionic Re_6 cluster and an appropriate amphiphilic ammonium cation, the formation of mesomorphic material could be expected. We report herein the synthesis via the ISA strategy and study of the first clustomesogen compound showing thermotropic and lyotropic behaviors.

EXPERIMENTAL SECTION

Experimental Techniques. NMR spectra were recorded on a Bruker Avance 300P. All peaks were referenced to the methyl signals of TMS at δ = 0 ppm. UV−Vis absorption measurements were performed on a Varian Cary 5000 UV−vis−NIR spectrophotometer. Luminescence spectra were recorded on a Fluorolog-3 fluorescence spectrometer (FL3−22, Horiba Jobin Yvon). Elemental analysis was performed in the CRMPO with a Microanalyser Flash EA1112 CHNS/O Thermo Electron. Energy-dispersive spectroscopy (EDS) was performed on a JEOL 6400 scanning electron microscope equipped with a XEDS Oxford field spectrometer. The electron paramagnetic resonance (EPR) spectrum was recorded on the powdered sample at 77K with a BRUKER EMX X-band spectrometer equipped with an Oxford cryostat. The transition temperatures and enthalpies were measured by differential scanning calorimetry (DSC) with a Perkin-Elmer Diamond instruments using a 10 °C/min scanning rates. Two or more heating−cooling cycles were performed on each sample. Mesomorphism was studied by hot stage polarizing microscopy using a Nikon 50i Pol microscope equipped with a Linkam THMS600 hot stage and a TMS94 temperature controller. Small-angle X-ray scattering (SAXS): X-ray diffraction patterns were collected with a Mar345 Image-Plate detector (Maresearch) mounted on a rotating anode X-ray generator FR591 (Bruker-AXS) operated at 50 kV and 50 mA with Cu Kα radiation (λ = 1.541 Å).[15] The sample to detector distance was calibrated by using silver behenate. The X-ray patterns were recorded for a range of reciprocal spacing $q = 4\pi\sin\theta/\lambda$ from 0.05 to 3.1 $Å^{-1}$ or 0.03−1.6 $Å^{-1}$, where θ is the diffraction angle. The experiments performed with the present setup provide accurate measurements of distances between 210 Å and 2 Å. The acquisition time was 3 h. The sample was loaded in a thin Lindemanm glass capillar (diameter 1.0 ± 0.1 mm and thickness 10 μm; GLAS, Muller, Berlin, Germany) and placed in a oven for thermotropic studies. The scattering intensities as a function of the radial wave vector were determined by circular integration.

Synthesis. $KCs_3[Re_6Se_8(CN)_6]$ and bis (w-[4-(4′-cyanobiphenylyl)oxy]decyl]dimethylammonium bromide (KAT-Br) were obtained by reported procedure with conform analytical data.[16] Starting materials were purchased from Acros, Alfa Aesar, and Aldrich, and used without further purification unless otherwise stated.

$KAT_3[Re_6Se_8(CN)_6]$ (1). To a brown-orange water solution of $KCs_3Re_6Se_8(CN)_6$ (0.08 g, 0.032 mmol of cluster in 5 mL of H_2O) was added 2 drops of liquid bromine. The solution turned green immediately and was stirred for 10 min at 25 °C. Addition of a solution containing KAT-Br in hot ethanol (0.076 g, 0.096 mmol in 5 mL of ethanol) induced the immediate formation of a light green precipitate. The mixture was refluxed for 1 h under stirring to complete the reaction, cooled to 25 °C and layered with dichloromethane. The organic phase was separated, dried over $MgSO_4$, and evaporated to give the desired product as a green compound. ^{1}H NMR (300 MHz, CD_2Cl_2): 1.18−1.87 (32 H, m), 3.28−3.48 (10 H, m), 4.0−4.1 (4 H, t), 7.0−7.1 (4 H, d), 7.55−7.60 (4 H, d), 7.67−7.74 (8 H, m). EDS:Re:Se 6:8.09, no bromine, no cesium, and no potassium. Elemental anal. C150 H186 N15 O6 Se8 Re6. Calcd: C, 44.55; H, 5.64; N, 5.19. Found: C, 44.55; H, 5.69; N, 4.93 .

$KAT_4[Re_6Se_8(CN)_6]$ (2). To a brown-orange water solution of $KCs_3Re_6Se_8(CN)_6$ (0.08 g, 0.032 mmol of cluster in 5 mL H_2O) was added a solution of KAT-Br in hot ethanol (0.103 g, 0.128 mmol in 5 mL). A light yellow precipitate formed immediately. The mixture was refluxed for one hour under stirring to complete the reaction. The desired compound was obtained by filtration, washed with water and hot ethanol 3 times and dried under vacuum. ^{1}H NMR (300 MHz, CD_2Cl_2): 1.2.-1.9 (32 H, m), 3.28−3.31 (10 H wide band), 3.99−4.04 (4 H, t), 6.99−7.02 (4 H, d), 7.45−7.55 (4 H, d), 7.66−7.73 (8 H, m). EDS: Re: Se 6: 8.09, no bromine, no cesium, and no potassium. Elemental analysis: C198 H248 N18 O8 Se8 Re6 calculated: C:49.99 ; H: 5.25 ; N: 5.30, found C: 49.62 ; H: 5.22, N: 5.26.

RESULTS AND DISCUSSION

Synthesis. Compounds **1** and **2** are made of $[Re_6Se_8(CN)_6]^{n-}$ clusters associated with dialkyldimethylammonium counter cations bearing cyanobiphenyloxy terminated alkyl chains (KAT^+, Scheme 1). The choice of this specific

Scheme 1. Schematic Representation of the Chemical Structure of $[Re_6Se_8(CN)_6]^{n-}$ and KAT^+ Countercation

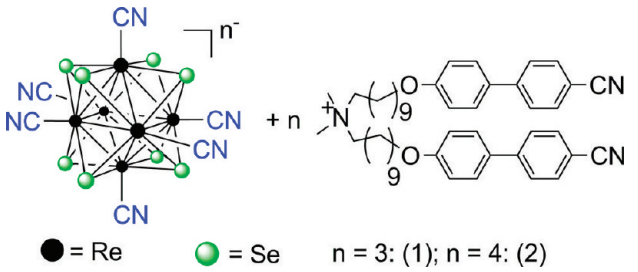

cation was driven by several considerations: i) according to Binnemans et al.[11b,17] double-tailed ammonium cations have to be preferred to monotailed ones to promote mesomorphic character in such hybrid assemblies. Indeed, in the case of $[Ni_3P_3S_{12}]^{3-}$ complexes, Camerel et al.[13] used double-tail dialkyldimethylammonium cations (with 12, 14, 16, or 18 carbon atom in the alkyl chains) to generate stable room temperature liquid-crystalline material. For bulkier inorganic species such as polyoxometalates, dialkyldimethylammonium containing biphenyl groups in the alkyl chains were used to generate lamellar mesomorphic phases;[12b] (ii) the cyanobiphenyl moiety is well-known to generate liquid crystal phases;

dx.doi.org/10.1021/cm201589d|Chem. Mater. 2011, 23, 5122−5130

and (iii) this cation was previously used to obtain bilayer vesicles in water. Although the same LC behavior for the hybrid is obviously not expected, as synergetic effects may occur between the organic and inorganic parts of the material, KAT-Br exhibits a monotropic thermotropic liquid crystalline phase of nematic type below 117 °C.[18]

KAT^+ was obtained as its bromide salt form according to reported procedure,[16] so as the cluster precursors $KCs_3[Re_6Se_8(CN)_6]$.[19] For this last one, cyano groups in apical position were preferred to halogen or hydroxo ones because of the high stability of the Re−CN bond and thus, to avoid any side reactions due to apical ligand exchange that may occur during the cationic metathesis process.[7j] Oxidized clusters $[Re_6Se_8(CN)_6]^{3-}$ were obtained by adding few drops of Br_2 in an aqueous/ethanol solution of $[Re_6Se_8(CN)_6]^{4-}$. The solution, initially bright orange, turns immediately to a dark green color characteristic of the oxidized cluster.

The desired products $(KAT)_3[Re_6Se_8(CN)_6]$ (**1**) and $(KAT)_4[Re_6Se_8(CN)_6]$ (**2**) were obtained by immediate precipitation when an ethanol solution containing a slight excess of the ammonium salt (KAT-Br) was added to a water solution of the cluster precursor.

The obtained solids were carefully washed successively with hot water and hot ethanol to remove the alkali salts and the unreacted organic ammonium salt. The exchange and purity of **1** and **2** were confirmed by energy-dispersive spectroscopy measurements (no traces of bromine or cesium could be detected), ^1H NMR, and elemental analysis.

Physicochemical Studies. To verify that the cluster core intrinsic properties were not or poorly affected by the cationic metathesis reaction, compounds were analyzed by several techniques such as absorption and emission spectroscopies, cyclic voltammetry and EPR measurements. Absorption spectroscopy studies realized on **1** and **2** show the typical UV−vis spectra of $[Re_6Se_8(CN)_6]^{n-}$ (n = 3, 4; Figure 1).[4b,20]

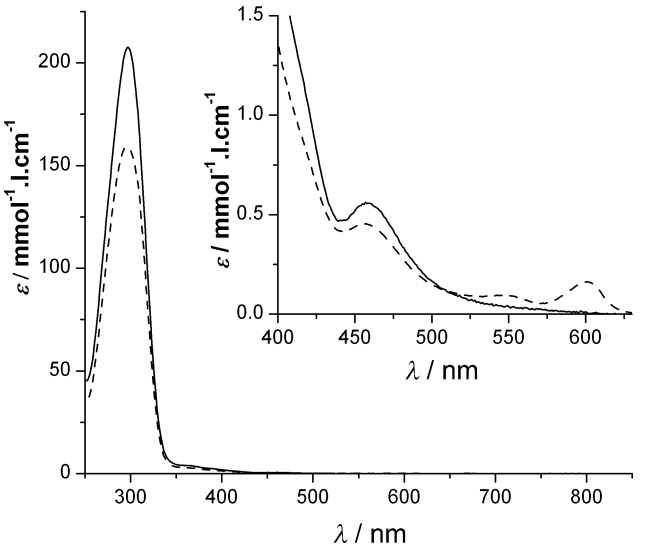

Figure 1. UV−vis spectra in CH_2Cl_2 of **1** (dashed line) and **2** (plain line).

These absorption spectra are composed of multiple absorption bands corresponding to ligand to metal charge transfer contributions from both inner and apical ligands that combine to form a broad and ill-resolved band in the 210−550 nm region. Depending on the charge of the cluster, significant color changes can be observed from orange (for n = 4) to dark green (for n = 3). These noticeable differences between the spectra demonstrate that a significant change in the electronic structure of the cluster anion occurs upon the one-electron oxidation. Note that oxidation suppresses the luminescence of the cluster moiety.

Cyclic voltammetry realized on **2** (Figure 2b) in CH_2Cl_2 (c = 3.2×10^{-4} mol L^{-1}, in a $(n\text{-}Bu_4N)PF_6$ 0.1 mol L^{-1} degassed solution), revealed a one electron reversible oxidation step located at $E^{0'}$ = 0.27 V vs SCE (ΔE_p = 110 mV) that is consistent with the $24e^-/23e^-$ oxidation process of the cluster core.[14] The paramagnetic character of **1** was demonstrated by EPR measurements realized at 77K (Figure 2a). The calculated g value (g = 2.55) is in the range of previously reported ones for hexanuclear rhenium cluster anions ($[Re_6Q_8L_6]^{3-}$ (Q = S, Se, Te ; L = CN, Cl, Br; 2.44−2.56)). The magnetic moment μ_{eff} = 2.2 μB of **1** is larger than the spin 1/2-only value (μSO = 1.73 μB) which is in agreement with a high spin−orbit coupling.[20a,21]

Luminescence properties of **2** were investigated in the solid state at room temperature on a sample deposited between two quartz slides and in a solution of dichloromethane (figure 2c). Indeed, rhenium cluster anions ($[Re_6Q_8L_6]^{4-}$) are known for exhibiting a red-NIR photoluminescence both in solution and in the crystalline phase. In both cases, irradiation anywhere in the absorption band (between 350 and 540 nm) induces the typical bright red-NIR phosphorescence of Re_6 clusters from 600 nm to nearly 900 nm. Gray et al.[4b] showed by combining spectroscopic, computational and photophysical studies, that the emissive state is not of ligand to metal charge transfer (LMCT) type but associated with the cluster core. They suggested that the LUMO−HOMO gap is insensitive to the nature of the apical ligands, owing to the dominant metal character of the HOMO and LUMO energy levels. Thus, this long-lived and bright luminescence may be obtained as long as the $[Re_6Q_8]^{2+}$ core is unperturbed, regardless of the nature of the apical ligands and a fortiori, regardless of the nature of its countercations.

This point confers to the cluster a major advantage compared to other inorganic emitting phosphors such as lanthanide cations or lanthanide containing polyoxometalates that emit in the same region. Indeed, in this last case, it has been shown recently by C. F. J. Faul et al.[22] that the luminescence properties of an europium containing polyoxometalate were strongly influenced by the nature of the organic countercation used. In fact, this functionality was simply suppressed when ferrocene containing cationic surfactants were used. The luminescence quantum yield of $[Re_6Se_8(CN)_6]^{4-}$ in degassed CH_2Cl_2 was found to be 0.115[4b] and no antennae is needed to improve their light absorption, as is usually the case for trivalent lanthanide cations.[23]

Therefore, all these observations confirm that the use of KAT^+ as countercation for 3^- and 4^- anionic cluster cores do not affect their intrinsic properties. Re_6 clusters can be reversibly switched from the bright red-NIR luminescent cluster form **2** to the green and magnetic one **1**.

Lyotropic Liquid Crystal Properties. As polyoxometalate surfactant materials,[22,24] compounds **1** and **2** show lyotropic phase behavior. Polarized photomicrographs of contact preparation with chloroform are presented in Figure 3. Compound **1** shows a texture of nematic type containing broad schlieren features along with large homeotropic areas, whereas **2** exhibits a marbled texture also of nematic type.[25] In

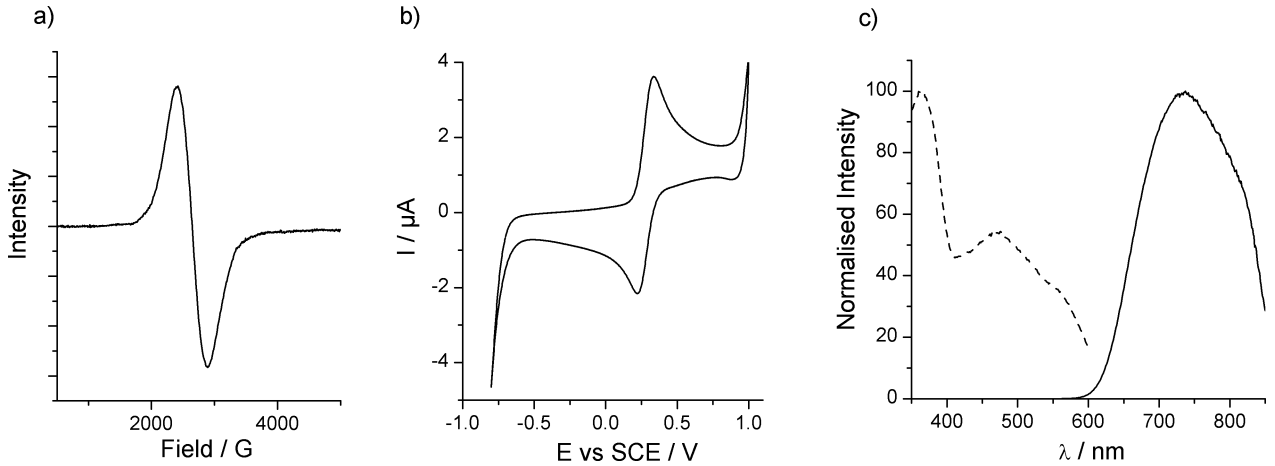

Figure 2. (a) EPR spectrum of compound (1) $[KAT]_3[Re_6Se_8(CN)_6]$ at 77 K; (b) cyclic voltammogram of **2** $[KAT]_4[Re_6Se_8(CN)_6]$ at $c = 3.2 \times 10^{-4}$ mol L^{-1} in a $(n\text{-}Bu_4N)PF_6$ 0.1 mol L^{-1} solution; (c) normalized excitation (dashed line, λ_{obs} = 700 nm) and emission (plain line, λ_{exc} = 440 nm) spectra of compound (2) $[KAT]_4[Re_6Se_8(CN)_6]$ taken in the solid state.

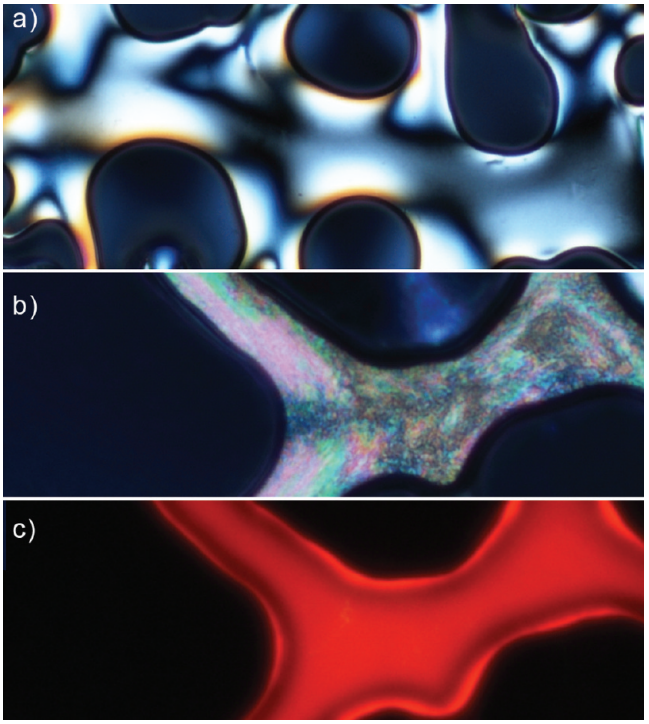

Figure 3. Optical textures of the lyotropic mesophase in chloroform at room temperature of (a) **1**, (b) **2** under normal light, and (c) **2** under irradiation with λ_{exc} = 405 nm.

addition, Figure 3c shows the bright red-NIR luminescence of **2** in its lyotropic mesophase. To confirm such behavior, we performed small-angle X-ray scattering (SAXS) studies on samples deposited in Lindemann capillary tubes and covered with chloroform. The solvent was allowed to slowly evaporate and diffraction patterns were recorded successively for two or three hours until complete evaporation. This set up allowed us to follow the self-organization process upon increasing concentration of **1** or **2**. Figure 4 shows representative 2D diffractograms, integrated patterns obtained successively during solvent evaporation as well as drawings illustrating the deduced supramolecular organization. From a general point of view, similar behaviors are observed for both compounds. At low concentration, large and diffuse scattering halo corresponding to a nematic order are observed. In the case of **1** (Figure 4a), this broad halo is centered around 34.6 Å and correspond to the size of the supramolecular species. Recently, S.-J. Kim et al.[26] obtained crystalline mesolamellar structures with $[Re_6Q_8(CN)_6]^{4-}$ (Q = Te, Se, S) clusters and commercially available monoalkyltrimethylammonium cations. They showed that the interlamellar distance could be tuned by varying the organic cation monoalkyl chain length, whereas the thickness of the inorganic layer containing the Re_6 clusters could be evaluated from crystallographic data to 12.255 Å. The length of KAT^+ in its full extended conformation was estimated by molecular means (Hyperchem software) to 25.5 Å.

Hence, depending on the cations position around the cluster anion, the length of KAT^+-Re_6 cluster assemblies can vary from 38 Å to 58 Å (see Figure S3). Yet, these values are slightly overestimated as the length of KAT^+ is taken in its full extended conformation and thus, we consider that a length of 34.6 Å is in good agreement with the average length of supramolecular entities.

For **2**, instead of a signal corresponding to the compounds length, two weak halos located with *d*-spacings of 20 and 10.3 Å could be guessed from the diffraction pattern (Figure 4c). These broad reflections reveal the tendency of Re_6 clusters to self-organize in monolayers as shown in the drawing of Figure 4c, which is compatible with the marbled texture observed by POM. Note that because of the long acquisition time and therefore solvent evaporation, a reflection corresponding to the d_{001} of the following lamellar organization (S) emerges from the baseline of the diffractogram. Indeed, decreasing the amount of solvent, induces the formation of layered phases that were not detected by POM, most probably because of the compounds high viscosity. Panels b and d in Figure 4 represent patterns of layered architectures for **1** and **2** respectively. These patterns contain each two sharp reflections in the reciprocal spacing ratio 1:2, corresponding to a lamellar periodicity (layer thickness) of d = 37.4 Å for **1** and d = 39.9 Å for **2**. Therefore, the introduction of a supplementary ammonium cation and thus, two more cyanobiphenyl mesogenic units, around the same cluster core has few influence on the interlayer distance. One could however expect more effects on the lateral organization and more particularly on the interclusters distance within the layers. For **1**, the broadness of the reflections relative to the lateral arrangement exclude any clear interpretation and

dx.doi.org/10.1021/cm201589d | *Chem. Mater.* 2011, 23, 5122–5130

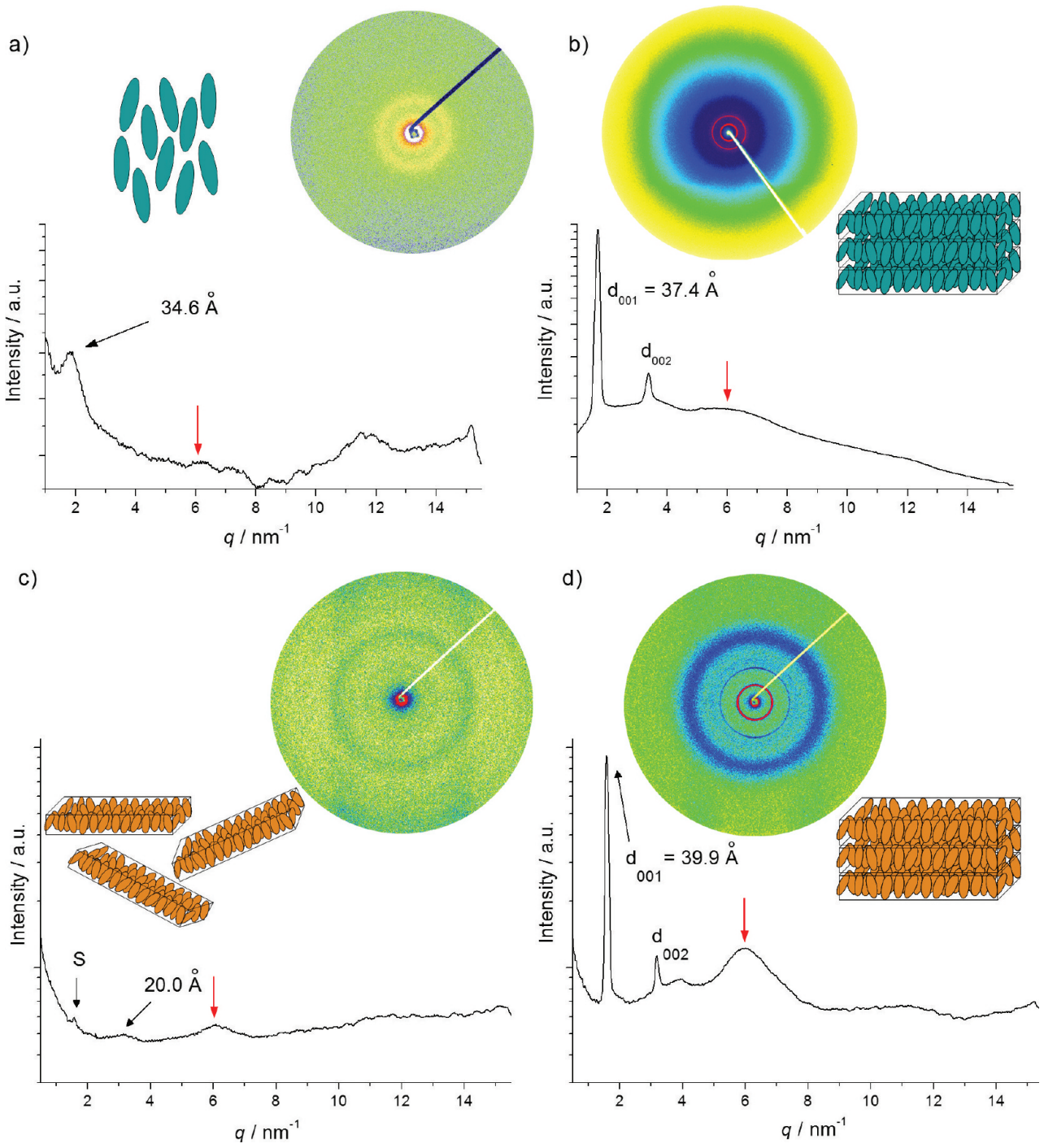

Figure 4. 2D and integrated SAXS diffraction patterns recorded successively at 20 °C upon slow evaporation of a $CHCl_3$ solution of (a, b) compound **1**, (c, d) compound **2**.

the mesophase was assigned to a smectic A. In the case of **2**, the broad reflections relative to the average inter cluster distance within the layer are enhanced compared to what was previously observed in figure 4c. The first reflection is located at q = 3.95 nm^{-1} and corresponds to a distance of 15.9 Å which gives an area per supramolecular species of approximately 200 $Å^2$. By considering that the mesogenic arms are equally distributed on both clusters sides, only a full interdigitation of the decyloxycyanobiphenyl moieties belonging to two successive layers gives a satisfactory transverse cross-section value for a cyanobiphenyl group (25 $Å^2$). This interdigitation is also supported by the small inter layer distance deduced from the two sharp signals. The second reflection located at q = 6.10 nm^{-1} is observed for both compounds either in the nematic (weak signal) or in the smectic (stronger signal) phases (red arrow in Figure 4). It corresponds to a periodicity d = 10.3 Å that is commonly found in the crystalline state for intercluster distance value.[26a,27] Its broadness reveals, in conjunction with the signal at q = 3.95 nm^{-1}, the disorder existing within the cluster layer that is typical for SmA phase. The full solvent evaporation induces the crystallization of **2**, whereas **1** retains its arrangement in a glassy state (see ESI for diffractograms).

dx.doi.org/10.1021/cm201589d | *Chem. Mater.* 2011, 23, 5122–5130

To the best of our knowledge, only one group reported the lyotropic behavior of octahedral metallic clusters.[28] However, in this case, the inorganic molecular species were condensed through triangular faces to form infinite conducting molecular wires of formula $[Mo_6Se_6]^{2-}$ with alkaly countercations.[29] Thus, the liquid crystalline behavior does not originate from synergetic effects between the anionic metallic part (which in our case can be considered as an isotropic molecular species) and its cationic counterpart, but more on the anisotropy of the inorganic specie itself. Authors of the study reported that $[Mo_6Se_6]^{2-}$ solutions (n-methylformamide or dimethylsulfoxide) are not stable for more than a few hours when in contact with dioxygen because of decomposition of the cluster chains. In our case, compounds are very stable and this is the first time that such lyotropic behavior is reported for molecular octahedral metallic clusters.

Thermotropic liquid crystal properties. The thermal properties of both compounds were first investigated by differential scanning calorimetry (DSC), and temperature-dependent POM. Thermal data are summarized in Table 1,

Table 1. Thermal Data for 1 and 2 Second Heating and First Cooling Cycle

compd	transition[a]	T (°C)	ΔH (kJ mol^{-1})
1	SmA-I	133	13.1
	I-SmA	139	10.7
	Tg	45	
2	Cr-I	153	33.4
	I-M	143	31.5[b]
	M-Cr		

[a]M = unidentified mesophase. [b]Combined enthalpy of the two transitions that could not be separated.

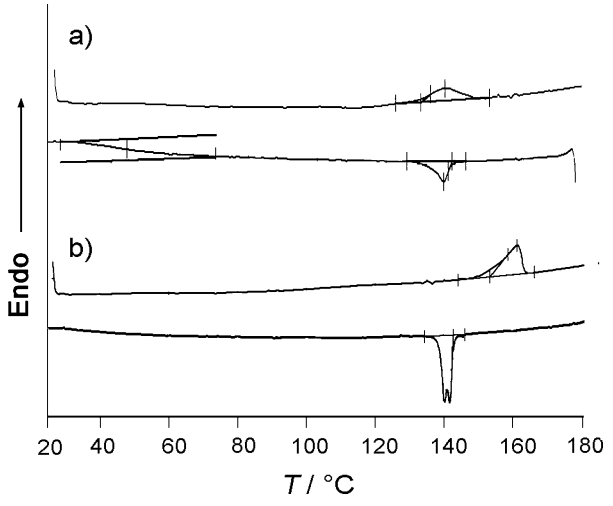

Figure 5. Comparison of DSC thermograms obtained for the first cooling (bottom curve) and second heating (top curve) cycles for (a) compound **1** and (b) compound **2**.

whereas DSC thermograms are presented in Figure 5. On cooling compound **1** from the isotropic liquid (figure 5a), one transition corresponding to the formation of a monotropic liquid crystalline phase could be detected at 140 °C on the DSC trace, followed by the formation of a glassy state around 45 °C.

During the second heating cycle, no crystallization peak was detected, and only one endothermal peak assigned to the isotropization process was seen which confirms the monotropic character of the mesophase. The transition between mesophase and isotropic state is perfectly reversible and the transition temperatures are kept constant during multiple heating–cooling cycles performed on the same sample. The enthalpy change (ΔH) associated to this transition is 10.7 kJ mol^{-1} which is higher than commonly found values for isotropic-liquid crystal transitions.[30] However, by considering that the mesomorphic character is essentially due to interactions between the organic cations, this value can be divided by three, giving thus an enthalpy value (3.57 kJ mol^{-1}) in the range of isotropic liquid–smectic liquid crystal transition.

For compound **2**, two endothermal peaks are observed during the first heating, one around 156 °C, corresponding to a transition between two crystalline forms while the second one, around 173 °C, corresponds to the transition to the isotropic state (ESI). On cooling from the isotropic liquid, the formation of a monotropic mesophase and its red luminescence under irradiation at 405 nm could be observed by POM (Figure 6).

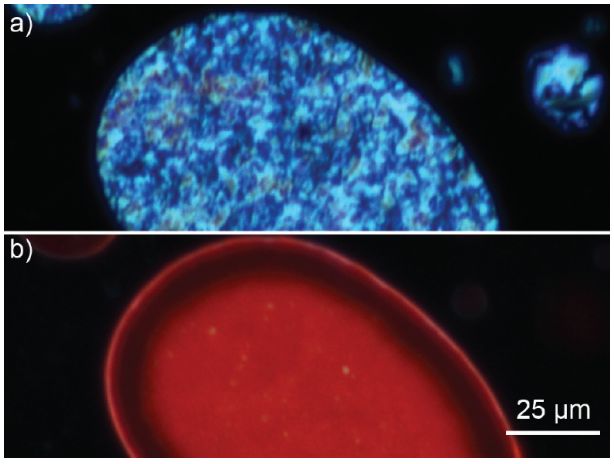

Figure 6. Polarized optical microphotograph of **2** (a) under normal light and(b) upon excitation (λ_{exc} = 405 nm) at 143 °C.

Unfortunately, crystallization occurs almost concomitantly, preventing the formation of a good and somehow reasonable to detect texture. This phenomenon is best seen on the DSC thermograms (Figure 5b), where two superimposed peaks are easily identified on cooling around 143 °C.

The texture developed by **1** from the isotropic liquid observed by POM at 137 °C contains homeotropic regions as well as features of a focal conic texture and is characteristic of a layered structure (Figure 7). Temperature dependent X-ray diffraction experiments were carried out in this case to identify the exact nature of the observed mesophase. Figure 8 shows the diffraction pattern obtained at 100 °C. All diffraction patterns recorded below this temperature were all qualitatively equivalent and contain three sharp small angle reflections characteristic of a highly ordered layered morphology with reciprocal spacing in the 1:2:3 ratio. By applying the Bragg's law, a spacing of 37.4 Å attributed to the interlayer distance was calculated. Note that this value is the same as the one found during the lyotropic studies.

dx.doi.org/10.1021/cm201589d|*Chem. Mater.* 2011, 23, 5122–5130

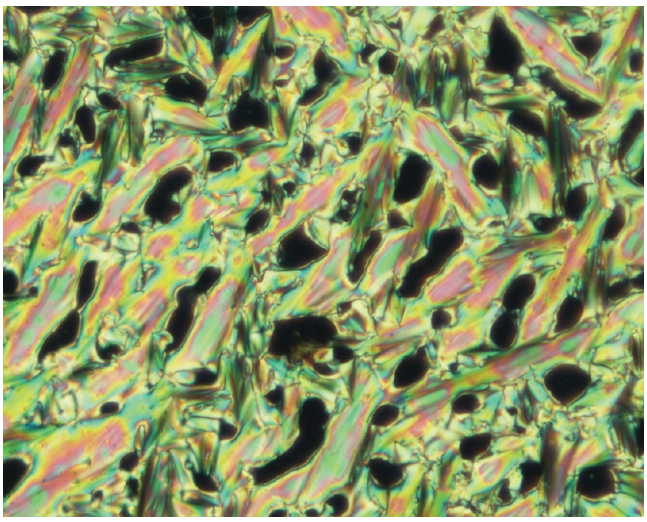

Figure 7. Polarized optical microphotograph of **1** observed at 100 °C.

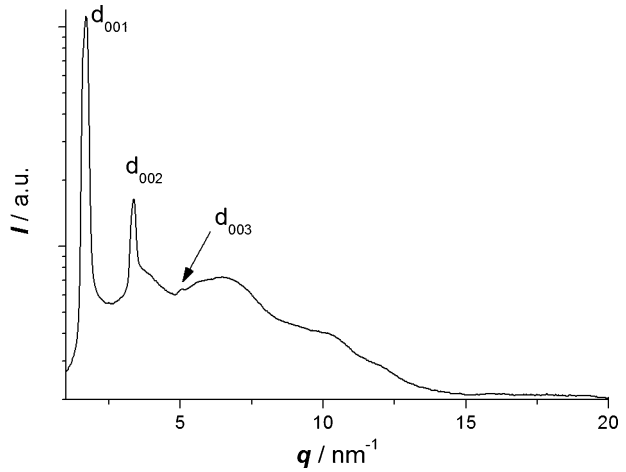

Figure 8. Temperature-dependent X-ray diffraction patterns at 100 °C obtained for **1**.

Besides the sharp reflections corresponding to the lamellar arrangement, additional very broad and intense reflections are observed and indicate some kind of local ordering within the electron rich Re_6 clusters layers. Note that M. J. Suh et al.[26a] reported a pseudo hexagonal packing of the clusters within the inorganic layer of their monocrystals. Although such arrangement could eventually be guessed from the position of the reflection maxima, the reflections broadness excludes any clear geometrical interpretation. Moreover, on the contrary of the inorganic crown-shaped $[Ni_3P_3S_{12}]^{3-}$, for which an hexagonal mesophase was evidenced once in presence of double-tail dialkyldimethylammonium surfactant,[13] the clusters isotropy excludes any type of preferential arrangement due to geometrical constraint. Therefore, the mesophase was attributed to a layered phase of Smectic A type with fully interdigitated organic cations as depicted in Figure 9. This interpretation is also in good accordance with the POM pictures obtained in the mesophase. Cooling down below the glass transition temperature had little effects on the X-ray diffraction pattern (a little increase in the interlayer distance was detected from 37.4 Å to 38.0 Å at 100 and 40 °C, respectively) showing that the layered morphology is retained.

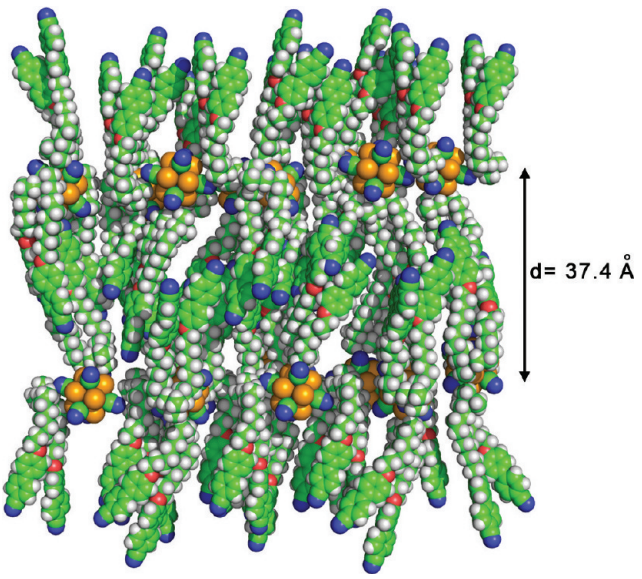

Figure 9. Illustration of the lamellar packing of **1** in the smectic A liquid crystal phase.

It is interesting to note that **1** and **2** show different thermotropic properties but behave in the same way after addition of a little amount of solvent. This may be explained by a modulation of the electrostatic interactions strength existing between the cationic ammonium heads and the isotropic anionic rhenium clusters. Indeed, in both cases, mesomorphic properties are driven predominantly by these electrostatic interactions, whereas weaker interactions between the cyanobiphenyl moieties promote the self-organization of the whole hybrid material. When solvent is added, solvatation of the anionic clusters minimizes the strength of the ammonium headgroup−anionic clusters electrostatic interactions. As a result, the contribution to the whole self-organization process of weaker interactions occurring between the cyanobiphenyl moieties increases, which induces the same lyotropic behavior for both compounds. The thermotropic studies show that isotropization of **1**(n = 3) and **2** (n = 4) occurs at 133 and 153 °C, respectively. This observation reveals that strong electrostatic interactions play a major role in stabilizing the thermotropic mesophase transition. As for surfactant encapsulated polyoxometalate,[12c] a higher charge of the cluster implies a more stable mesophase. Another important feature of **1** and **2** is that their thermotropic LC-isotropic state transition temperature is reached much before the compound's degradation temperature and moreover below 200 °C. This should prevent, for applications purposes, the decomposition of the semiconductor and/or substrate, and more particularly organic flexible substrate, during any annealing processes. Note that such behavior is unusual for LC materials obtained via the ISA strategy. Indeed, as discussed recently by C. F. J. Faul et al.,[31] this type of compounds usually degrades before reaching the isotropic state and to the best of our knowledge, **1** and **2** are the first example of switchable functional ISA LC material behaving in such a way.

CONCLUSIONS

We have demonstrated in this work that the ionic self-assembly approach is an easy alternative to the covalent way to generate self-organized materials containing transition metal cluster either by a simple heating and cooling process or by addition of

dx.doi.org/10.1021/cm201589d | Chem. Mater. 2011, 23, 5122–5130

little amount of solvent. Indeed, by combining a dialkyldimethylammonium cation containing cyanobiphenyl moieties terminated alkyl chains with an anionic $[Re_6Se_8(CN)_6]^{3-}$ cluster, a thermotropic lamellar smectic A liquid crystalline phase is obtained. Lyotropic nematic and smectic liquid crystalline mesophases were also observed independently of the cluster charge. We have also shown that the intrinsic properties of the molecular inorganic cluster are preserved within the mesomorphic material. It is therefore possible to switch reversibly this LC material from a green-colored magnetic form to a bright red-NIR luminescent one. These compounds, because of their low clearing temperature, can be integrated and annealed directly in devices. Yet that the concept of such class of material is demonstrated, the endless range of possibilities offered by organic chemists to design particular mesogenic cations allowing a fine-tuning of the final material mesomorphic behavior, associated with the versatility of the inorganic clusters (charge, functions) obtained via high-temperature solid-state synthesis, open new and fascinating perspectives in the design of easy processable functional material containing transition metal clusters.

■ ASSOCIATED CONTENT

Ⓢ Supporting Information

Luminescence spectrum in solution of **2**; X-ray diffraction patterns and DSC thermograms. This material is available free of charge via the Internet at http://pubs.acs.org.

■ AUTHOR INFORMATION

Corresponding Author

*E-mail: yann.molard@univ-rennes1.fr.

■ ACKNOWLEDGMENTS

Financial support for this work was provided by UR1, PHC Brancusi 19616UF, PECO-NEI 370, PICS 5822 (RFBR 11-03-91052) (2011-2013) Programs, and Region Bretagne (CREATE Program, M.A.-C.). The authors thank T. Guizouarn for EPR, Y. Le Gal for voltammetry, and Dr. V. Marchi Artzner for access to the spectrofluorimeter.

■ REFERENCES

(1) (a) Bruce, D. W.; Dunmur, D. A.; Lalinde, E.; Maitlis, P. M.; Styring, P. *Nature* **1986**, *323* (6091), 791. (b) Giroud-Godquin, A. M.; Maitlis, P. M. *Angew. Chem., Int. Ed.* **1991**, *30* (4), 375. (c) Donnio, B.; Guillon, D.; Deschenaux, R.; Bruce, D. W. Metallomesogens. In *Comprehensive Coordination Chemistry II: From Biology to Nanotechnology*; Mc Cleverty, J. A., Meyer, J. J., Fujita, M., Powell, A., Eds.; Elsevier: Oxford, U.K., 2003; Vol. 7, pp 357. (d) Binnemans, K. *J. Mater. Chem.* **2009**, *19* (4), 448.

(2) (a) Molard, Y.; Dorson, F.; Circu, V.; Roisnel, T.; Artzner, F.; Cordier, S. *Angew. Chem., Int. Ed.* **2010**, *49* (19), 3351. (b) Mocanu, A. S.; Amela-Cortes, M.; Molard, Y.; Circu, V.; Cordier, S. *Chem. Commun.* **2011**, *47*, 2056.

(3) Date, R. W.; Iglesias, E. F.; Rowe, K. E.; Elliott, J. M.; Bruce, D. W. *Dalton Trans.* **2003**, No. 10, 1914.

(4) (a) Gray, T. G.; Rudzinski, C. M.; Nocera, D. G.; Holm, R. H. *Inorg. Chem.* **1999**, *38* (26), 5932. (b) Gray, T. G.; Rudzinski, C. M.; Meyer, E. E.; Holm, R. H.; Nocera, D. G. *J. Am. Chem. Soc.* **2003**, *125* (16), 4755. (c) Kitamura, N.; Ueda, Y.; Ishizaka, S.; Yamada, K.; Aniya, M.; Sasaki, Y. *Inorg. Chem.* **2005**, *44* (18), 6308.

(5) Maverick, A. W.; Najdzionek, J. S.; MacKenzie, D.; Nocera, D. G.; Gray, H. B. *J. Am. Chem. Soc.* **1983**, *105* (7), 1878.

(6) Maverick, A. W.; Gray, H. B. *J. Am. Chem. Soc.* **1981**, *103* (5), 1298.

(7) (a) Long, J. R.; Williamson, A. S.; Holm, R. H. *Angew. Chem., Int. Ed. Engl.* **1995**, *34* (2), 226. (b) Cordier, S.; Kirakci, K.; Mery, D.; Perrin, C.; Astruc, D. *Inorg. Chim. Acta* **2006**, *359* (6), 1705. (c) Ababou-Girard, S.; Cordier, S.; Fabre, B.; Molard, Y.; Perrin, C. *ChemPhysChem* **2007**, *8* (14), 2086. (d) Grasset, F.; Dorson, F.; Cordier, S.; Molard, Y.; Perrin, C.; Marie, A.-M.; Sasaki, T.; Haneda, H.; Bando, Y.; Mortier, M. *Adv. Mater.* **2008**, *20* (1), 143. (e) Grasset, F.; Dorson, F.; Molard, Y.; Cordier, S.; Demange, V.; Perrin, C.; Marchi-Artzner, V.; Haneda, H. *Chem. Commun.* **2008**, *39*, 4729. (f) Grasset, F.; Molard, Y.; Cordier, S.; Dorson, F.; Mortier, M.; Perrin, C.; Guilloux-Viry, M.; Sasaki, T.; Haneda, H. *Adv. Mater.* **2008**, *20* (9), 1710. (g) Shestopalov, M. A.; Cordier, S.; Hernandez, O.; Molard, Y.; Perrin, C.; Perrin, A.; Fedorov, V. E.; Mironov, Y. V. *Inorg. Chem.* **2009**, *48* (4), 1482. (h) Fabre, B.; Cordier, S.; Molard, Y.; Perrin, C.; Ababou-Girard, S.; Godet, C. *J. Phys. Chem. C* **2009**, *113* (40), 17437. (i) Aubert, T.; Grasset, F.; Mornet, S.; Duguet, E.; Cador, O.; Cordier, S.; Molard, Y.; Demange, V.; Mortier, M.; Haneda, H. *J. Colloid Interface Sci.* **2010**, *341* (2), 201. (j) Aubert, T.; Ledneva, A. Y.; Grasset, F.; Kimoto, K.; Naumov, N. G.; Molard, Y.; Saito, N.; Haneda, H.; Cordier, S. *Langmuir* **2010**, *26* (23), 18512.

(8) Cotton, F. A. *Inorg. Chem.* **1964**, *3* (9), 1217.

(9) Long, J. R.; McCarty, L. S.; Holm, R. H. *J. Am. Chem. Soc.* **1996**, *118* (19), 4603.

(10) (a) Selby, H. D.; Roland, B. K.; Zheng, Z. *Acc. Chem. Res.* **2003**, *36* (12), 933. (b) Mery, D.; Plault, L.; Nlate, S.; Astruc, D.; Cordier, S.; Kirakci, K.; Perrin, C. Z. *Anorg. Allg. Chem.* **2005**, *631* (13−14), 2746. (c) Mery, D.; Plault, L.; Ornelas, C.; Ruiz, J.; Nlate, S.; Astruc, D.; Blais, J. C.; Rodrigues, J.; Cordier, S.; Kirakci, K.; Perrin, C. *Inorg. Chem.* **2006**, *45* (3), 1156. (d) Szczepura, L. F.; Ketcham, K. A.; Ooro, B. A.; Edwards, J. A.; Templeton, J. N.; Cedeno, D. L.; Jircitano, A. *J. Inorg. Chem.* **2008**, *47* (16), 7271. (e) Prabusankar, G.; Molard, Y.; Cordier, S.; Golhen, S.; Le Gal, Y.; Perrin, C.; Ouahab, L.; Kahlal, S.; Halet, J. F. *Eur. J. Inorg. Chem.* **2009**, *14*, 2153. (f) Molard, Y.; Dorson, F.; Brylev, K. A.; Shestopalov, M. A.; Le Gal, Y.; Cordier, S.; Mironov, Y. V.; Kitamura, N.; Perrin, C. *Chem.—Eur. J.* **2010**, *16* (19), 5613.

(11) (a) Faul, C. F. J.; Antonietti, M. *Adv. Mater.* **2003**, *15* (9), 673. (b) Binnemans, K. *Chem. Rev.* **2005**, *105* (11), 4148. (c) Faul, C. F. J. *Mol. Cryst. Liquid Cryst.* **2006**, *450*, 255.

(12) (a) Yin, S. Y.; Li, W.; Wang, J. F.; Wu, L. X. *J. Phys. Chem. B* **2008**, *112* (13), 3983. (b) Li, W.; Yin, S. Y.; Wang, J. F.; Wu, L. X. *Chem. Mater.* **2008**, *20* (2), 514. (c) Li, W.; Yi, S. Y.; Wu, Y. Q.; Wu, L. X. *J. Phys. Chem. B* **2006**, *110* (34), 16961.

(13) Camerel, F.; Antonietti, M.; Faul, C. F. J. *Chem.—Eur. J.* **2003**, *9* (10), 2160.

(14) Yoshimura, T.; Ishizaka, S.; Sasaki, Y.; Kim, H. B.; Kitamura, N.; Naumov, N. G.; Sokolov, M. N.; Fedorov, V. E. *Chem. Lett.* **1999**, *10*, 1121.

(15) Van Grondelle, W.; Iglesias, C. L.; Coll, E.; Artzner, F.; Paternostre, M.; Lacombe, F.; Cardus, M.; Martinez, G.; Montes, M.; Cherif-Cheikh, R.; Valery, C. *J. Struct. Biol.* **2007**, *160* (2), 211.

(16) Everaars, M. D.; Marcelis, A. T. M.; Sudholter, E. J. R. *Langmuir* **1993**, *9* (8), 1986.

(17) Slougui, A.; Mironov, Y. V.; Perrin, A.; Fedorov, V. E. *Croat. Chem. Acta* **1995**, *68* (4), 885.

(18) Everaars, M. D.; Marcelis, A. T. M.; Sudholter, E. J. R. *Langmuir* **1996**, *12* (16), 3964.

(19) Mironov, Y. V.; Cody, J. A.; AlbrechtSchmitt, T. E.; Ibers, J. A. *J. Am. Chem. Soc.* **1997**, *119* (3), 493.

(20) (a) Guilbaud, C.; Deluzet, A.; Domercq, B.; Molinie, P.; Coulon, C.; Boubekeur, K.; Batail, P. *Chem. Commun.* **1999**, *18*, 1867. (b) Naumov, N. G.; Ostanina, E. V.; Virovets, A. V.; Schmidtman, M.; Muller, A.; Fedorov, V. E. *Russ. Chem. Bull.* **2002**, *51* (5), 866.

(21) Larina, T. V.; Ikorskii, V. N.; Vasenin, N. T.; Anufrienko, V. F.; Naumov, N. G.; Ostanina, E. V.; Fedorov, V. E. *Russ. J. Coord. Chem.* **2002**, *28* (8), 554.

(22) Zhang, T. R.; Liu, S. Q.; Kurth, D. G.; Faul, C. F. J. *Adv. Funct. Mater.* **2009**, *19* (4), 642.

(23) (a) Binnemans, K. *Chem. Rev.* **2009**, *109* (9), 4283. (b) Bunzli, J. C. G. *Chem. Rev.* **2010**, *110* (5), 2729.

(24) Zhang, T. R.; Spitz, C.; Antonietti, M.; Faul, C. F. J. *Chem.—Eur. J.* **2005**, *11* (3), 1001.
(25) Li, W.; Zhang, J.; Li, B.; Zhang, M. L.; Wu, L. X. *Chem. Commun.* **2009**, *35*, 5269.
(26) (a) Suh, M. J.; Vien, V.; Huh, S.; Kim, Y.; Kim, S. J. *Eur. J. Inorg. Chem.* **2008**, *5*, 686. (b) Huh, S.; Suh, M. J.; Vien, V.; Kim, Y.; Hwang, S. J.; Kim, S. J. *Small* **2009**, *5* (10), 1123. (c) Vien, V.; Suh, M. J.; Huh, S.; Kim, Y.; Kim, S. J. *Chem. Commun.* **2009**, *5*, 541.
(27) Naumov, N. G.; Virovets, A. V.; Fedorov, V. E. *J. Struct. Chem.* **2000**, *41* (3), 499.
(28) Davidson, P.; Batail, P.; Gabriel, J. C. P.; Livage, J.; Sanchez, C.; Bourgaux, C. *Prog. Polym. Sci.* **1997**, *22* (5), 913.
(29) Potel, M.; Chevrel, R.; Sergent, M. *J. Solid State Chem.* **1980**, *35* (2), 286.
(30) Singh, S. *Phys. Rep.—Rev. Sec. Phys. Lett.* **2000**, *324* (2—4), 108.
(31) Zhang, T.; Brown, J.; Oakley, R. J.; Faul, C. F. J. *Curr. Opin. Colloid Interface Sci.* **2009**, *14* (2), 62.